

PACS 52.77.Dq, 73.61.Ey, 73.61.Jc, 78.40.Pg, 78.66.Fd

## Structure and optical properties of AlN films obtained using the cathodic arc plasma deposition technique

A.P. Shapovalov<sup>1</sup>, I.V. Korotash<sup>1</sup>, E.M. Rudenko<sup>1\*</sup>, F.F. Sizov<sup>2</sup>, D.S. Dubyna<sup>1</sup>, L.S. Osipov<sup>1</sup>,  
D.Yu. Polotskiy<sup>1</sup>, Z.F. Tsybrii<sup>2</sup>, A.A. Korchovy<sup>2</sup>

<sup>1</sup>*G.V. Kurdyumov Institute for Metal Physics, NAS of Ukraine,  
36, Academician Vernadsky Blvd., 03680 Kyiv, Ukraine,*

*Phone/fax: +38(044) 424-3432; \*e-mail: rudenko@imp.kiev.ua*

<sup>2</sup>*V. Lashkaryov Institute of Semiconductor Physics, NAS of Ukraine,  
41, prospect Nauky, 03028 Kyiv, Ukraine,*

*Phone/fax: +38(044) 525-6296, e-mail: sizov@isp.kiev.ua*

**Abstract.** Aluminum nitride (AlN) film coatings have been obtained by a new technique of hybrid helikon-arc ion-plasma deposition. Possibility to combine the magnetic-filtered arc plasma deposition technique with a treatment in RF plasma of helicon discharge allowed us to deposit AlN coatings on thermolabile substrates, significantly increasing the deposition rate. A study of spectral properties of AlN films (reflection and transmission spectra within the range 2...25  $\mu\text{m}$ ) has been carried out by using the infrared Fourier spectrometer Spectrum BX-II. It has been shown that the obtained composite structures (AlN coatings on teflon and mylar substrates) could be used as passive filters in the infrared spectral range.

**Keywords:** AlN films, coatings on polymeric materials, optical properties, cathodic arc plasma deposition technique.

Manuscript received 19.11.14; revised version received 19.03.15; accepted for publication 27.05.15; published online 08.06.15.

### 1. Introduction

Over the past few years, a number of group III metal nitrides (AlN, InN and GaN, etc.) have been attracting considerable attention of researchers as objects for the fundamental study, and also as base materials for optoelectronics [1-4]. AlN coatings demonstrate a huge potential for their application in high-power electronic devices. Similar to  $\text{Al}_2\text{O}_3$  and  $\text{HfO}_2$ , AlN has a high dielectric constant, low dielectric losses and high breakdown voltage. Therefore, it is typically used as a gate dielectric or an insulating layer responsible for the

elimination of parasitic currents [5, 6]. Furthermore, AlN is one of the few non-metallic solids with high thermal conductivity (up to 320 W/m·K at 25 °C) [6]. These properties make AlN a very promising material for absorption and conduction of the heat generated in microelectronic devices. At the same time, aluminum nitride has a high chemical resistance and good mechanical properties (hardness of ~18 GPa) [7].

To obtain AlN films, conventional deposition techniques such as alternating (AC) and direct current (DC) reactive magnetron sputtering, laser ablation, molecular beam epitaxy (MBE) and many others have

been widely used [8-14]. In comparison with these techniques, a cathodic arc plasma deposition technology with magnetic filtration of plasma flow, which has been developing by the authors, has certain advantages associated with universality of the method, low temperature of the deposition process and high rate of coatings condensation. In contrast to standard "BULAT" type industrial facility for cathodic arc plasma deposition, our original combined facility allows us to carry out an efficient separation of a droplet component of the sputtering flow from the end surface of the cathode, using magnetic system with a bent configuration of the magnetic field. A magnetic filtration allows us to achieve a high content of the high-energy (15 to 50 eV) ionic component in the plasma flow directed to a substrate, as well as to separate the microdroplet component. The temperature of the synthesis of dense films under such conditions could be reduced down to the room one. The control of the position of the deflected flow through an adjustment of the current of magnetic system and substrate rotation system enables us to achieve uniform coatings on samples with the diameter up to 150 mm.

The possibility to combine this technique with specific features of the helicon source of RF-plasma treatment gave us an opportunity to realize AlN films deposition on various substrates, including the thermolabile ones (different polymers) and to carry out the study of structural and optical properties of films obtained.

To improve characteristics of radio astronomy receivers, production of barrier filters in the middle infrared (mid-IR) spectral range is required. At the same time, these filters must be fabricated on dielectric materials, which are traditionally used in the microwave technology. Typically, this polymer material is Teflon that has a low thermal conductivity (down to 0.25...1 W/m·K at 25 °C). As have been shown by our research, a possible solution for this problem could be combination of dielectric materials with high and low thermal conductivity.

This paper presents results of the synthesis and study of AlN film coatings on thin flexible thermolabile polymer substrates (teflon and mylar) and on single-crystal silicon substrates (*n*-Si). The structure of AlN films has been studied. Transmission and reflection spectra of composite structures "AlN film on a substrate" have been obtained in the mid-IR spectra (2 to 25 μm). It has been shown that composite structures "AlN film on the polymer substrate" could have characteristics of barrier filter in the mid-IR spectra.

## **2. Experimental techniques for obtaining and study of AlN films**

To obtain AlN films on various substrates, an original combined ion-plasma facility based on helicon and magnetic-filtered arc plasma sources (MFAPS) was used [15]. Technological chamber of the reactor consists of a

discharge chamber of the helicon source (with diameter and height of 20 cm) and a drift chamber (with diameter of 35 cm and height of 25 cm). A discharge was excited by planar antenna with diameter of 11 cm, which was connected via a device matching to the RF generator with the frequency of 13.56 MHz and with the power up to 1 kW in the presence of argon or a reactive gas at the pressure close to 7...8 mTorr. The MFAPS module was attached to the end of the drift chamber. The substrate holder, in which the electric potential could vary within the range 0...100 V was placed at the bottom of the drift chamber. A more detailed description of our facility could be found in Ref. [15].

It is known that teflon is chemically inert, and adhesion of metal films to its surface is hindered due to the low surface energy (saturated bonds of fluorine on the surface). As was shown in Ref. [16], a significant increase in adhesion of metal films to the teflon surface could be achieved through a pre-sputtering of the substrate surface by an ion beam before deposition. We used this method to provide the adhesion of AlN films to all our substrates. The following operations were carried out without breaking the vacuum, consecutively: 1) treatment of the sample surface by plasma of the helicon source at different potentials of a substrate in an inert argon atmosphere; 2) film deposition on various substrates, using magnetic-filtered arc plasma sources. A single crystal silicon *n*-Si (100) and (111), as well as polymeric films of mylar and teflon were used as substrates. The use of single crystal substrates allowed us to carry out model experiments for the study of structural and optical properties of coatings. The use of polymeric films of mylar and teflon as substrates allowed us to estimate real potentiality of AlN coatings for producing quasi-optical passive infrared (IR) filters.

The crystal structure of samples was studied by using the X-ray diffractometer (XRD) STADIP (Stoe, Germany) with copper radiation  $\text{Cu}_{K\alpha}$ . Angles at which shooting of XRD patterns was carried out ranged between 20° and 90°. To average the intensity of X-ray reflection from a single-crystal substrate and a film on it, the sample was rotated during the shooting around the axis perpendicular to its plane. Surface morphology of the films was investigated using the scanning probe microscope NanoScope IIIa Dimension 3000™ in the mode with the periodic contrast. Measurements were carried out in the central area of samples by means of serial silicon probes (NT-MDT, Russia) with the nominal tip radius of 10 nm.

Reflection and transmission spectra in the mid-IR spectral range were obtained by using the IR Fourier spectrometer Spectrum BX-II (Perkin Elmer) based on a single-beam scanning interferometer Dynascan with a Ge/KBr beam distributor. A signal was recorded using the DTGS-detector. The spectral resolution of the device was not worse than 0.8  $\text{cm}^{-1}$ , and the signal/noise ratio was higher than 15000/1. Built-in Sure Scan checking system provided reliability of the performed measurements.

### 3. Study of the structure inherent to the prepared AlN films

For the AlN films deposition, such single crystal substrates as *n*-Si (100) and (111) were used. According to the International Centre for Diffraction Data, the following values of the position of main reflexes of AlN films in the diffraction pattern were obtained, using  $\text{Cu}_{K\alpha 1}$  radiation with  $\lambda = 0.15406 \text{ nm}$ : (100) AlN –  $33.36^\circ$ , (002) AlN –  $35.91^\circ$  and (101) AlN –  $38.03^\circ$ , with the relative intensity of reflections 999, 606 and 914, respectively. Fig. 1 shows the XRD pattern of the AlN film deposited on the *n*-Si (100) substrate (curve 2), in which no other reflections were observed except the substrate ones (curve 1). We note the increase of the background in the area of small angles, which indicates the presence of an amorphous component in the film structure. However, we could not unambiguously exclude the presence of a crystalline phase, since the (200) reflection of the *n*-Si substrate, which was at  $33.2^\circ$  could coincide with the position of the (100) AlN reflection ( $33.36^\circ$ ). Fig. 2 shows the XRD pattern of the AlN film deposited on the *n*-Si (111) substrate, in which all the main reflections of aluminum nitride films ((100) AlN, (002) AlN and (101) AlN) are present. At the same time, grains of (002) and (101) orientations are clearly dominated. It should be noted that nucleation conditions in the case of the deposition on the *n*-Si (100) substrate will differ significantly from those in the case of the deposition on the *n*-Si (111) one. Thus, we could assume predominance of (100) AlN grains.

The study of surface morphology inherent to the AlN films revealed a dense developed film surface, which is typical for the condensation under significant bombardment of growing condensate by high-energy particles of plasma. As one can see in Fig. 3a, rounded-shape nanosize grains are distributed uniformly over the test area. Fig. 3b shows that the average height difference between adjacent grains is 1.5...2.5 nm. At the same time, Fig. 3c shows the statistical histogram of average distances between the peaks in the range between 30 and 50 nm.

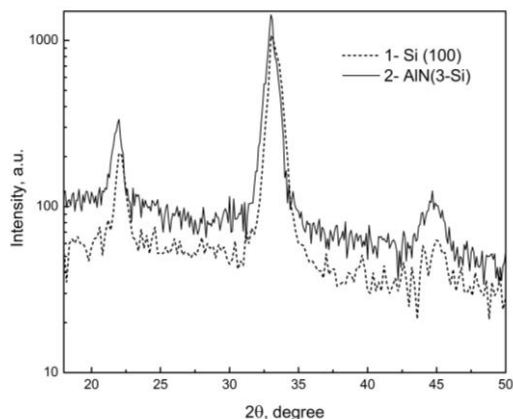


**Fig. 1.** XRD patterns of the AlN film deposited on the *n*-Si (100) (2) and *n*-Si (100) substrate (1).

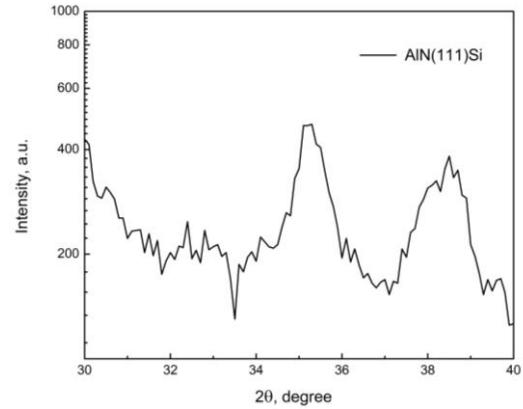
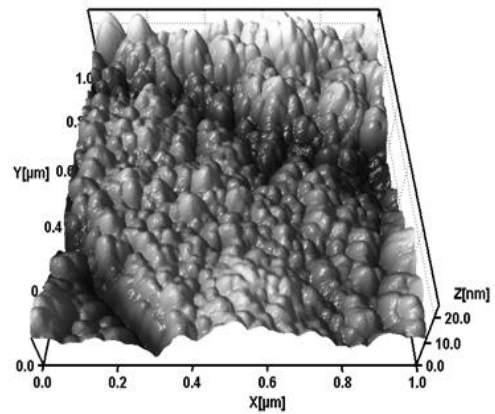
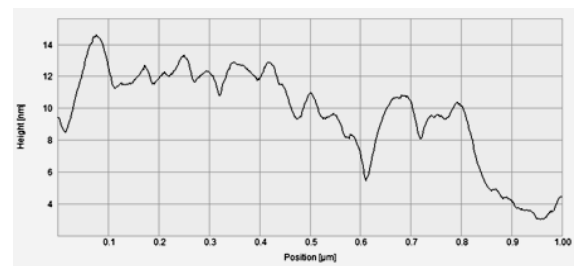


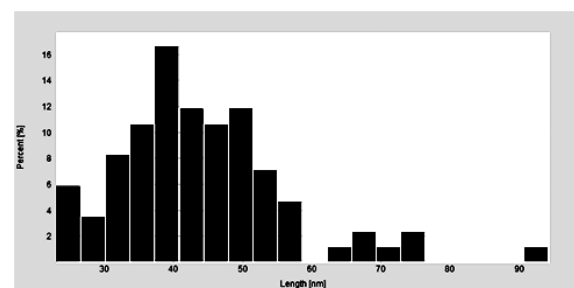
**Fig. 2.** XRD pattern of the AlN film deposited on the *n*-Si (111).



a)



b)



c)

**Fig. 3.** Three-dimensional image (a), cross-sectional profile (b) and histogram of distance distribution (c) of the AlN film, which were obtained using the scanning probe microscope NanoScope IIIa Dimension 3000™.

#### 4. Spectral properties of composite structures in the mid-IR spectra

The study of the reflection and transmission spectra for the composite structures of AlN films and obtained substrates were carried out in the mid-IR spectra for the wavelengths in the range from 2 to 25  $\mu\text{m}$ . Further, for the samples obtained we will use the following notations: AlN (3-Si) is the AlN film with the thickness 3.3  $\mu\text{m}$  deposited on the *n*-Si (100) substrate with the thickness 0.4 mm; AlN (4-myl) – the AlN film with the thickness 4.2  $\mu\text{m}$  on the mylar substrate with the thickness 40  $\mu\text{m}$ ; AlN (8-myl) – the AlN film with the thickness 8.5  $\mu\text{m}$  on the mylar substrate with the thickness 40  $\mu\text{m}$ ; AlN (8-tefl) – the AlN film with the thickness 8.5  $\mu\text{m}$  on the teflon substrate with the thickness 0.1 mm. Fig. 4 shows four reflection spectra (for the selected scale  $\text{cm}^{-1}$ ), the interference pattern for curves that correspond to AlN (4-myl) and AlN (3-Si) samples is more readable).

According to the laws of classical optics [17], the relationship between a film thickness ( $d$ ), refractive index of the material of a film ( $n(\lambda)$ ), and values of radiation wavelengths ( $\lambda_1, \lambda_2$ ) for which adjacent maximum (or minimum) are observed in the interference pattern, is determined as

$$d = \frac{\lambda_1 \lambda_2}{2[n(\lambda_2)\lambda_1 - n(\lambda_1)\lambda_2]} \quad (1)$$

If we neglect the dependence of the refractive index  $n(\lambda)$  on the wavelength and use the average value of  $n$ , the expression (1) could be re-written as:

$$d = \frac{\lambda_1 \lambda_2}{2n(\lambda_1 - \lambda_2)} \quad (2)$$

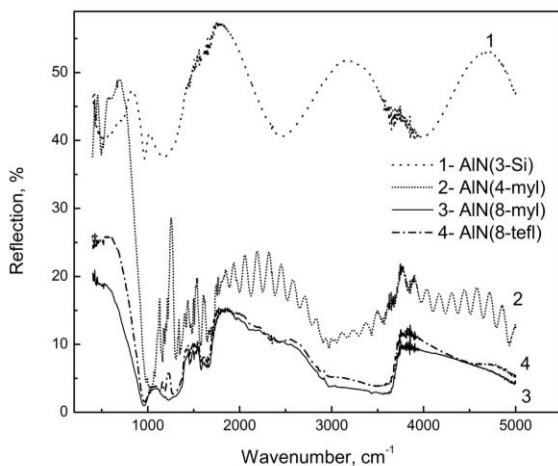


**Fig. 4.** The reflection spectra obtained for the samples (1) AlN (3-Si), (2) AlN (4-myl), (3) AlN (8-myl), (4) AlN (8-tefl) in the mid-IR spectral region.

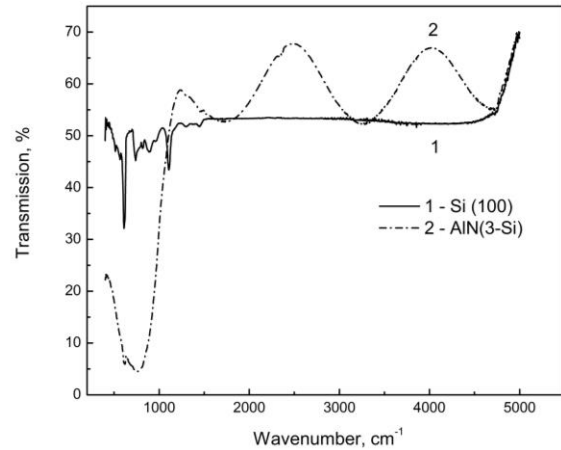


**Fig. 5.** The transmission spectra obtained for the *n*-Si (100) silicon substrate (1) and the AlN (3-Si) structure (2) in the mid-IR spectral region.

As one can see in Fig. 4, the interference pattern is clearly observed in two curves: (1) – AlN (3-Si) and (2) – AlN (4-myl). Moreover, overlaying of two interference patterns with different repetition periods occurs in the curve (2) – AlN (4-myl). The longer period is associated with interference in the AlN film thickness and with less repetition period in the underlayer of mylar. We could estimate the film thickness using the formula (2) and the refractive index of the AlN film ( $n = 1.928$ ) obtained in Ref. [18], which was averaged in the wavelength range 2.5 to 7.3  $\mu\text{m}$ . Substituting values of wavelengths  $\lambda_1, \lambda_2$  for two adjacent maxima and minima into (2), we obtain the following values of film thicknesses:  $d = 3.26 \mu\text{m}$  and  $d = 3.39 \mu\text{m}$ , respectively. The difference in the values associated with a dispersion of the refractive index of the AlN film  $n$ , i.e. for more accurate calculations we should use the formula (1) instead of (2).

Fig. 5 shows the transmission spectra with transparency values for the *n*-Si (100) substrate and the AlN (3-Si) sample. The characteristic absorption band associated with a transverse optical (TO) vibration of AlN bonds is present in the IR spectrum of the AlN(3-Si) structure obtained. Broadening this band and the shift ( $\sim 705 \text{ cm}^{-1}$ ) in comparison with that for crystalline AlN ( $\sim 670 \text{ cm}^{-1}$ ) is typical for amorphous films and could be associated with the presence of impurities in the form of oxygen and carbon in the AlN films structure. We note that outside the absorption band in the more high-energy part of the spectrum of the AlN (3-Si) structure, an effect of translucency is observed. An increase in the transparency of the composite structure in comparison with the transparency of the silicon substrate could be associated with an increase in the AlN film roughness. Analyzing the interference pattern, we could note that the position of maxima and minima in accordance with classical optics remains the same, but now they are swapped.

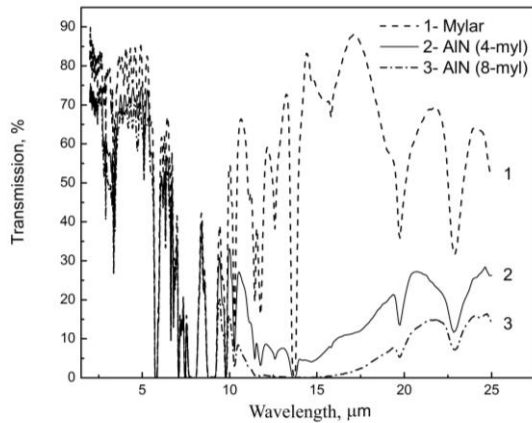


**Fig. 6.** The transmission spectra obtained for the mylar substrate (1) and the AIN (4-myl) (2) and AIN (8-myl) (3) structures in the mid-IR spectral region.

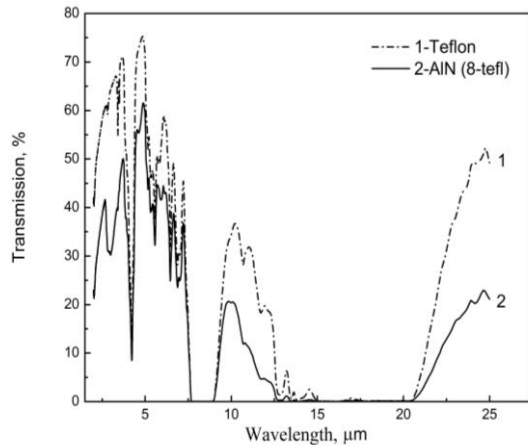


**Fig. 7.** The transmission spectra obtained for the teflon substrate (1) and the AIN (8-tefl) (2) in the mid-IR spectral region.

Figs. 6 and 7 show the comparative transmission spectra of substrates (mylar with the thickness 40  $\mu\text{m}$  and teflon with the thickness 100  $\mu\text{m}$ ) as well as composite structures of these substrates and AIN films. It should be noted that in the entire range (2...25  $\mu\text{m}$ ), the AIN amorphous film (with the thickness 4 to 8  $\mu\text{m}$ ) improves properties of our composite structures obstructing IR radiation (especially within the range 7.5 to 25  $\mu\text{m}$ ). The latter range determines the thermal radiation band of bodies heated to room temperatures.

To estimate the efficiency of coatings obtained, let us introduce the integrated transmission coefficient  $T_{a-b}$  for the AIN (4-myl); AIN (8-myl); AIN (8-tefl) composite structures as well as mylar and teflon substrates (before deposition). The integrated transmission coefficient  $T_{a-b}$  could be found from the formula:

$$T_{a-b} = \frac{1}{(b-a)} \int_a^b T_x dx, \quad (3)$$

**Table. Integrated transmission coefficients  $T_{7.5-25}$  and extinction coefficients  $K_{ext}$  for the composite structures obtained.**

	Mylar	AIN (4-myl)	AIN (8-myl)	Teflon	AIN (8-tefl)
$T_{7.5-25}$ (%)	63.40	12.46	4.42	7.31	2.89
$K_{ext}$	1.00	0.20	0.07	1.00	0.40

where  $a$  and  $b$  are limits of the spectral range studied (in our case,  $a = 7.5 \mu\text{m}$  and  $b = 25 \mu\text{m}$ ). Also, we introduce the extinction coefficient  $K_{ext}$  that is equal to the ratio of the integrated transmission coefficient  $T_{7.5-25}$  of the composite structure to the integrated transmission coefficient  $T_{7.5-25}$  of its substrate. The results of  $T_{7.5-25}$  and  $K_{ext}$  estimations are given in Table. Taking into account a high thermal conductivity of AIN films, the results obtained are an evidence of possible application of these composite structures (AIN coatings on teflon and mylar substrates) as passive filters in the IR spectral range.

## 5. Conclusions

Technology for producing nano-disperse dense films of aluminum nitride on various substrates, including thermolabile polymeric films such as mylar and teflon by magnetic-filtered cathodic arc plasma deposition technique, has been developed. We provided a high level of adhesion to chemically inert surfaces of polymeric films by modifying the substrate surface through the pre-sputtering in the RF-plasma of helicon discharge. The low temperature mode of dense films deposition has been provided by high-energy plasma particles, which are emitted during the cathodic arc plasma deposition. The complex of physical characteristics such as low level of dielectric losses, high-level absorption in the infrared spectral range and improved thermal conductive properties provides the aluminum nitride coating-polymer film (mylar or teflon) composite structures with functional parameters necessary for producing quasi-optical filter elements in the infrared spectral region.

The value of attenuation of IR radiation depends on the AIN film thickness. Thus, deposition of AIN coating with the thickness 4.2  $\mu\text{m}$  on the mylar film (with the thickness 40  $\mu\text{m}$ ) increased attenuation in the composite structure "AIN film on the mylar substrate" by not less than 5 times in the 7.5 to 25  $\mu\text{m}$  range, while AIN coating with the thickness 8.5  $\mu\text{m}$  increased attenuation by not less than 14 times in comparison with attenuation in the mylar film within the same spectral range.

Deposition of AIN coating with the thickness 8.5  $\mu\text{m}$  on the teflon film (with the thickness 100  $\mu\text{m}$ ) increased attenuation in the composite structures "AIN film on the teflon substrate" by not less than 2.5 times in comparison with attenuation in the teflon film.

The obtained results have shown that such thermolabile polymeric films with AlN nanosize grains coatings can be used for suppressing the noise level from the background IR radiation within the range of 7.5 to 25  $\mu\text{m}$  to improve characteristics of sub-THz and THz receivers. Also, these AlN coatings on thermolabile polymeric films are applicable for perceptibility decrease of the objects radiation in the same spectral range.

#### References

1. S.C. Jain, M. Willander, J. Narayan and R. Van Overstraeten, III-nitrides: Growth, characterization, and properties // *J. Appl. Phys.* **87**(3), p. 965-1006 (2000).
2. S. Strite and H. Morkoç, GaN, AlN, and InN: A review // *J. Vac. Sci. Technol. B*, **10**(4), p. 1237-1266 (1992).
3. S.N. Mohammad, H. Morkoç, Progress and prospects of group-III nitride semiconductors // *Progress in Quantum Electronics*, **20**(5-6), p. 361-525 (1996).
4. K. Kubota, Y. Kobayashi and K. Fujimoto, Preparation and properties of III-V nitride thin films // *J. Appl. Phys.* **66**(7), p. 2984-2988 (1989).
5. K.S.A. Butcher and T.L. Tansley, Ultrahigh resistivity aluminum nitride grown on mercury cadmium telluride // *J. Appl. Phys.* **90**(12), p. 6217-6221 (2001).
6. D.D.L. Chung, Materials for thermal conduction // *Appl. Therm. Eng.* **21**(16), p. 1593-1605 (2001).
7. I. Yonenaga, Thermo-mechanical stability of wide-bandgap semiconductors: high temperature hardness of SiC, AlN, GaN, ZnO and ZnSe // *Physica B: Condens. Matt.* **308-310**, p. 1150-1152 (2001).
8. I. Ivanov, L. Hultman, K. Järrendahl, et al., Growth of epitaxial AlN(0001) on Si(111) by reactive magnetron sputter deposition // *J. Appl. Phys.* **78**(9), p. 5721-5726 (1995).
9. C.T.M. Ribeiro, F. Alvarez and A.R. Zanatta, Structural properties of aluminum-nitrogen films prepared at low temperature // *Appl. Phys. Lett.* **81**(6), p. 1005-1007 (2002).
10. D. Manova, P. Huber, S. Mändl, B. Rauschenbach, Filtered arc deposition and implantation of aluminium nitride // *Surface and Coatings Technology*, **142-144**, p. 61-66 (2001).
11. Y.F. Lu, Z.M. Ren, T.C. Chong, B.A. Cheong, S.K. Chow and J.P. Wang, Ion-assisted pulsed laser deposition of aluminum nitride thin films // *J. Appl. Phys.* **87**(3), p. 1540-1542 (2000).
12. Y. Watanabe and Y. Nakamura, Influence of ion beam irradiation on crystallographic structure and surface morphology of aluminium nitride thin films // *Ceram. Intern.* **24**(6), p. 427-432 (1998).
13. J.-W. Soh, S.-S. Jang, I.-S. Jeong, W.-J. Lee, C-axis orientation of AlN films prepared by ECR PECVD // *Thin Solid Films*, **279**(1-2), p. 17-22 (1996).
14. R.Y. Krupitskaya and G.W. Auner, Optical characterization of AlN films grown by plasma source molecular beam epitaxy // *J. Appl. Phys.* **84**(5), p. 2861-2865 (1998).
15. V.F. Semenuk, E.M. Rudenko, I.V. Korotash et al., Unified technological ion-plasma facility for formation of nanostructures // *Metallofizika i Noveishie Tekhnologii*, **33**(2), p. 223-231 (2011), in Russian.
16. C.A. Chang, Enhanced Cu-Teflon adhesion by presputtering treatment: Effect of surface morphology changes // *Appl. Phys. Lett.* **51**(16), p. 1236-1238 (1987).
17. T.S. Moss, G.J. Burrell, B. Ellis, *Semiconductor Opto-electronics*. Mir, Moscow, 1976 (in Russian).
18. N.S. Zayats, V.G. Boiko, P.A. Gentsar, O.S. Litvin, V.P. Papusha, N.V. Sopinskii, Optical study of AlN-n-Si(100) films obtained by RF magnetron sputtering technique // *Fizika i Tekhnika Poluprovodnikov*, **42**(2), p. 195-198 (2008), in Russian.